Pathogenic variants in *SQOR* encoding sulfide:quinone oxidoreductase are a potentially treatable cause of Leigh disease

Marisa W. Friederich[1,2], Abdallah F. Elias[3], Alice Kuster[4,5], Lucia Laugwitz[6], Austin A. Larson[1], Aaron P. Landry[7], Logan Ellwood-Digel[1], David M. Mirsky[8], David Dimmock[9], Jaclyn Haven[3], Hua Jiang[1], Kenneth N. MacLean[1], Katie Styren[3], Jonathan Schoof[3], Louise Goujon[4,10], Thomas Lefrancois[11], Maike Friederich[1], Curtis R. Coughlin II[1], Ruma Banerjee[7], Tobias B. Haack[5,12], Johan L.K. Van Hove[1,2,*]

1. Section of Clinical Genetics and Metabolism, Department of Pediatrics, University of Colorado, Aurora, Colorado, USA

2. Department of Pathology and Laboratory Medicine, Children's Hospital Colorado, 13121 East 16th Avenue, Aurora, Colorado, USA

3. Department of Medical Genetics, Shodair Children's Hospital, Helena, Montana, USA

4. Department of Neurometabolism, University Hospital of Nantes, Nantes, France

5. INRAE, UMR1280, PhAN, Nantes Université, Nantes, France

6. Institut für Medizinische Genetik und Angewandte Genomik, Universitätsklinikum, University of Tübingen, Tübingen, Germany

7. Department of Biological Chemistry, University of Michigan, Ann Arbor, Michigan, USA

8. Department of Radiology, University of Colorado, and Children's Hospital Colorado, Aurora, Colorado, USA

This is the author manuscript accepted for publication and has undergone full peer review but has not been through the copyediting, typesetting, pagination and proofreading process, which may lead to differences between this version and the Version of Record. Please cite this article as doi: 10.1002/jimd.12232

9. Rady Children's Institute for Genomic Medicine, Rady Children's Hospital, San Diego, California, USA

10. Service de Génétique Clinique, University Hospital of Rennes, Rennes, France

11. Pediatric Radiology, University Hospital of Nantes, Nantes, France

12. Centre for Rare Diseases, University of Tübingen, 72076 Tübingen, Germany

* corresponding author

Corresponding author:

Johan L.K. Van Hove, MD, PhD, MBA

Department of Pediatrics, Section of Clinic Genetics and Metabolism

University of Colorado

Education 2 South, L28-4114

13121 East 17th Avenue

Aurora, 80045, USA

Tel. 303-724-2365

Fax 720-777-7322

Email: Johan.Vanhove@childrenscolorado.org

Abbreviated title: Sulfide:quinone oxidoreductase disorder

Abstract

Purpose: Hydrogen sulfide, a signaling molecule formed mainly from cysteine, is catabolized by sulfide:quinone oxidoreductase (gene *SQOR*). Toxic hydrogen sulfide exposure inhibits complex IV. We describe children of two families with pathogenic variants in *SQOR*.

Methods: Exome sequencing identified variants; SQOR enzyme activity was measured spectrophotometrically, protein levels evaluated by western blotting, and mitochondrial function was assayed.

Results: In Family A, following a brief illness, a four-year-old girl presented comatose with lactic acidosis and multiorgan failure. After stabilization, she remained comatose, hypotonic, had neuro-storming episodes, elevated lactate, and Leigh-like lesions on brain imaging. She died shortly after. Her eight-year-old sister presented with a rapidly fatal episode of coma with lactic acidosis, and lesions in the basal ganglia and left cortex. Muscle and liver tissue had isolated decreased complex IV activity, but normal complex IV protein levels and complex formation. Both patients were homozygous for c.637G>A, which is a founder mutation in the Lehrerleut Hutterite with a carrier frequency of 1 in 13. The resulting p.Glu213Lys change disrupts hydrogen bonding with neighboring residues, resulting in severely reduced SQOR protein and enzyme activity, whereas sulfide generating enzyme levels were unchanged.

In Family B, a boy had episodes of encephalopathy and basal ganglia lesions. He was homozygous for c.446delT and had severely reduced fibroblast SQOR enzyme activity and protein levels.

Conclusion: SQOR dysfunction can result in hydrogen sulfide accumulation, which, consistent with its known toxicity, inhibits complex IV resulting in energy failure. SQOR deficiency represents a new, potentially treatable, cause of Leigh disease.

Take home message: Pathogenic variants in *SQOR* cause Leigh disease due to inhibition of respiratory chain enzyme complex IV by accumulation of hydrogen sulfide.

Contributions:

Study concept and design: JVH and MWF

Patient care data: JVH, AFE, AK, AAL, JH, DMM, LG, TL

Molecular data: MWF, AFE, LL, DD, KS, JS, MF, CRR, TBH, JVH

Laboratory studies: MWF, APL, LED, HJ, KNM, RB

First draft writing: MWF, JVH

Critical rewriting: MWF, AFE, DMM, DD, KNM, CRR, RB, TBH, JVH

Leadership and funding: MWF, AFE, KNM, RB, TBH, JVH

Final responsibility and guarantor: JVH

Corresponding author: Johan L.K. Van Hove

Competing interest statement:

JVH and AAL participate in clinical trials of mitochondrial disorders by Stealth Biotherapeutics, Inc. All other authors deny any real or apparent conflict of interest in the field of mitochondrial diseases.

Funding: Financial support for this study was received from Children's Hospital Colorado Foundation, Summits for Samantha and Miracles for Mito (JVH, MWF, AAL). The study was also supported by the NIH grants R35GM130183 to RB, and F32GM122357 to APL, and by NIH/NCATS Colorado CTSA Grant Number UL1 TR002535. LED was the recipient of a Child Health Research Internship at the CU Anschutz campus, which is supported by the Daniel and Janet Mordecai Foundation, Department of Pediatrics and the Research Institute, Children's Hospital Colorado. KNM gratefully acknowledges financial support from the William R. Hummel Homocystinuria Research Fund and holds the Ehst-Hummel-Kaufmann Family Endowed Chair in Inherited Metabolic Disease. Sequencing performed at the University of Colorado was performed by the Molecular Biology Unit of the Barbara Davis Center for BioResources Core Facility, which receives support from the Children's Diabetes Foundation, the Davis Trust, and the UC-AMC Strategic Infrastructure for Research Committee. TBH was supported by the German Bunderministerium für Bildung und Forsung (BMBF) through the Juniorverbund in der Systemmedizin "mitOmics" (FKZ 01ZX1405C to TBH), the intramural fortune program (#2435-0-0) and by the Deutsche Forschungsgemeinschaft (DFG, German Research Foundation) – Projektnummer (418081722). The Montana Genetics Program at Shodair Children's Hospital is supported by the Montana Department of Public Health and Human Services (PHH18-0157JT MT Clinical Genetics Program). Funding sources had no role in the design or execution of the study, the interpretation of data, or the writing of the study.

Ethics approval: Studies at the University of Colorado were done following IRB-approved protocols 07-0386 and 16-0146. Studies at Shodair Children's Hospital in Montana were done according to IRB-approved protocol IRB00008287. For studies of identifiable living human subjects, written informed

consent was obtained prior to initiation of research as outlined in the IRB-approved study. The study was approved by the ethics committee of the University of Tuebingen (437/2018BO1).

IACUC: No animals were used in this study.

Key words: Leigh disease, hydrogen sulfide, complex IV, treatment, sulfide:quinone oxidoreductase

INTRODUCTION

Despite the purported role of hydrogen sulfide (H_2S) as a signaling molecule with multiple physiologic functions, few inherited disorders have been described involving its metabolism or function[1,2]. Here we describe a new disorder of H_2S metabolism.

In brain, H_2S increases cAMP, stimulates NMDA-receptor mediated responses including long-term potentiation, and stimulates calcium influx in astrocytes. In the vascular system it promotes vasodilatation and angiogenesis[1,2]. It upregulates antioxidant systems, anti-inflammatory, and cytoprotective genes.

The toxicity of excess H_2S, such as occurs during exposure in industrial accidents, results in part from inhibiting cytochrome c oxidase, including by coordination with the iron of heme a[3]. It changes the ventilatory drive possibly by inhibiting carbonic anhydrase, and can cause pulmonary edema and cardiac depression. Chronic H_2S accumulation has been implicated in ethylmalonic encephalopathy and related to inhibition of short chain acyl-CoA dehydrogenase and loss of cytochrome c oxidase[4-7]. Finally, H_2S has been implicated in the pathophysiology of primary coenzyme Q deficiency[8,9].

The metabolism of H_2S is complex (Figure 1). At physiological pH, hydrogen sulfide consists of dissolved gaseous H_2S in equilibrium with HS^-. It is primarily generated from cysteine via the activity of three enzymes. In most tissues, the majority of H_2S production is derived via α,β-elimination by cystathionine

γ-lyase (*CTH*) upon L-cysteine to form L-serine and H_2S[10,11]. Also, H_2S is formed in the condensation reaction of cystathionine β-synthase (*CBS*) when L-serine is substituted by L-cysteine. Further, L-cysteine is transaminated by cysteine aminotransferase (CAT) with α-ketoglutarate forming 3-mercaptopyruvate, which is then acted upon by mercaptopyruvate sulfurtransferase (*MPST*) to release H_2S in mitochondria and in the cytosol[12]. In the brain, D-cysteine can be oxidized by D-amino-oxidase to mercaptopyruvate, the substrate for MPST[12]. Finally, gut bacteria produce H_2S, which is rapidly metabolized in the intestinal epithelium[7,13,14,15].

H_2S is primarily oxidized via sulfide:quinone oxidoreductase, an inner mitochondrial membrane protein encoded by the *SQOR* gene (previously called *SQRDL*) (OMIM# 617658). A cysteine persulfide is transiently formed in the SQOR active site while electrons from H_2S oxidation reduce coenzyme Q via the cofactor FAD[16]. The sulfane sulfur from this persulfide intermediate is then transferred to the physiological acceptor glutathione forming glutathione persulfide (GSSH). *In vitro*, sulfite, cyanide and other acceptors can substitute for glutathione forming thiosulfate, thiocyanate, and other products[17]. Glutathione persulfide is oxidized by persulfide dioxygenase (encoded by the gene *ETHE1,* pathogenic variants in this gene are implicated in ethylmalonic encephalopathy) to sulfite, which can be further oxidized to sulfate by sulfite oxidase or metabolized by thiosulfate sulfurtransferase to thiosulfate[7].

Leigh disease is a frequent neurologic presentation of genetic defects in mitochondrial bioenergetics[19]. It is highly heterogenous genetically with more than 75 causative genes identified, yet the genetic cause for many patients remains unresolved[20]. Most patients have defects in structural genes of the

respiratory chain complex, or in processes involving transcription, translation, or assembly of the protein complexes including their multiple cofactors. Defects in complex IV are a recurring cause of Leigh disease[21]. Very few mitochondrial disorders are related to secondary toxic inhibition of respiratory chain enzyme complexes. Few mitochondrial disorders have an effective treatment option.

Here we present children from two families who developed Leigh disease. The genetic defect was identified in the *SQOR* gene, and functional assays show abrogated SQOR enzyme activity and isolated decreased complex IV activity, but normal complex IV protein levels and complex formation. Recognition of this new genetic cause of Leigh disease is clinically important as it identifies a potentially treatable condition.

METHODS

Subjects

All procedures were done in accordance with the ethical standards of the ethics committee in accordance with the Helsinki Declaration of 1975 and as revised in 2000. Informed consent was obtained from all living subjects included in the study. The clinical histories were reviewed by clinical geneticists, and brain magnetic resonance imaging (MRI) studies were reviewed by a pediatric neuroradiologist (DM).

Exome sequencing

Exome sequencing was performed on the index cases and their parents. For an initial estimate of the carrier rate in the Hutterite population, de-identified DNA samples from this population that had been previously submitted for diagnostic studies for variable indications were screened by high resolution melt curve analysis and Sanger sequencing as described in Supplemental Methods. The carrier incidence in the general population was identified from the gnomAD database using a methodology as described in Supplemental methods[22].

Analysis of respiratory chain enzyme activities and assembly

Respiratory chain enzyme activities of complexes I, II, II+III, III, IV and citrate synthase were analyzed in duplicate in post-600x g supernatants isolated from liver and muscle of subject A.II-3 and from fibroblasts of subject B.II-3 as described previously[23]. Ratios of enzyme activities to either citrate synthase or complex II activities were calculated and expressed as Z-scores of the normal distribution established in control samples. Solubilized inner mitochondrial membrane fractions isolated by differential centrifugation from liver and muscle from subject A.II-3 and from fibroblasts from subject B.II-3 were separated by blue native polyacrylamide gel electrophoresis (BN-PAGE) and evaluated by in-gel activity staining assays as described previously[23].

Complex IV assembly was analyzed in isolated mitochondrial membrane fractions obtained from liver and muscle from subject A.II-3 using non-denaturing clear native PAGE followed by western blot analysis using the antibody against COXIV. Complex I assembly was analyzed in mitochondrial membrane fractions using non-denaturing BN-PAGE followed by western blot analysis using the antibody against

NDUFS2, as described previously[24]. In control samples, this assay shows only a holocomplex at 1 MDa and a faint band at 400 kDa in muscle samples, or at 230 kDa in fibroblasts.

Western blot analysis of mitochondrial proteins including SQOR

In subject A.II-3, complex IV integrity was evaluated using an antibody against COXIV and complex I integrity was evaluated using and antibody against NDUFB8 on western blot analysis. The amount of SQOR protein was determined by western blot analysis on mitochondrial inner membrane fractions. The levels of H_2S generating enzymes were evaluated by western blot analysis using antibodies to CBS, CTH, MPST, and cysteine dioxygenase (CDO). All methods are described in Supplemental Methods, and the source and specifications of all antibodies used are listed in Supplemental Table 1.

.

Analysis of SQOR enzyme activity in liver, blood cells, and fibroblasts

The activity of SQOR was measured spectrophotometrically in mitochondrial membrane fractions isolated from liver and in lysates derived from peripheral blood mononuclear cells (PBMC) and from fibroblasts as previously described for purified protein with the modifications described in detail in Supplemental Methods[26]. The reaction uses sulfite as acceptor, following coenzyme Q_1 reduction spectrophotometrically for 5-8 min at 278 nm. The kinetic parameters for human SQOR enzyme were evaluated in human liver and fibroblast samples.

Protein modeling, purification and *in vitro* characterization of the human SQOR mutant

The *SQOR* variant was mapped on the crystal structure of the human SQOR protein (PDB: 6O1C)[27] using PyMol[28]. The human SQOR mutant protein p.Glu213Lys was purified as reported previously for the wild type enzyme[17] and the absorption spectrum and concentration estimated as described in Supplemental Methods.

RESULTS

Case Reports

Family A. The proband, subject II-3, was a four-year-old girl born to consanguineous Lehrerleut Hutterite parents, whose grandparents were first cousins (Figure 2A). She had a history of recovering slower from infections than her siblings, but otherwise had no health concerns including no gastrointestinal symptoms. At onset of the illness, during the day she was more tired and vomited, and in the evening became rapidly encephalopathic with an episode of tonic seizures. Upon presentation, she was comatose with seizure-like movements, and Kussmaul breathing due to lactic acidosis with pH 6.86, anion gap 31, lactate 17.3 mM, and uric acid 7.8 mg/dL. She developed shock, respiratory insufficiency evolving into acute respiratory distress syndrome (ARDS), and multi-organ failure including liver failure with increased prothrombin time INR 1.76 and decreased clotting factors V and VII, mild hypoglycemia 47 mg/dL, mild hyperammonemia 112 µM, hypoalbuminemia 2.9 g/L, but normal cortisol. With supportive therapy, the multiorgan failure stabilized rapidly over the next days, but coma (Glasgow coma scale (GCS) 5, decorticate posturing) without further seizures, hypoalbuminemia (2.0 to 2.4 g/dL, normal 3.5-5.2 g/dL) with otherwise normal liver function (transaminases AST 52-88, normal 15-50), and lactic acidosis (3 to 5 mM with lactate/pyruvate ratio 17 and cerebrospinal fluid (CSF) lactate 3.0 mM)

persisted. Creatine kinase peaked at 722 U/L and remained mildly elevated. In subsequent weeks, she had generalized hypotonia, and episodes of neuro-storming with tachycardia, hypertension, and potentially pain, partially responding to treatment with phenobarbital, levetiracetam, baclofen, diazepam and propranolol. She also developed a thrombus in the right iliac to femoral vein requiring anticoagulation. She died a few days after discharge.

Workup for infectious agents and toxins was negative. The acylcarnitine profile, carnitine levels, 3-methylglutaconic acid, thiamin pyrophosphate level, and plasma, urine and CSF amino acids levels were all normal. Urine organic acids showed evidence of lactic acidosis and ketosis. The electroencephalogram showed diffuse slowing and lack of reactivity but no epileptiform activity, and full cardiac evaluation including echocardiogram was normal. Brain MRI on the fourth day of illness showed T2 prolongation and diffusion restriction in the caudate, putamina and globi pallidi (Figure 3A-B, white arrowheads). There was also diffusion restriction in the posterior part of the hippocampi (figure 3B white arrows), medial left temporal lobe, posterior inferior thalamus and the mammillary bodies (Figure 3C, white notched arrowheads). Further, there was increased T2 and FLAIR signal in the cerebral peduncles, dentate nuclei, and medial thalami, but brain stem, cerebellum, cortex and white matter were normal. Brain magnetic resonance spectroscopy (MRS) over the right basal ganglia showed a large lactate peak 6 times larger than the choline peak with a depressed N-acetylaspartate peak. Biopsies of muscle and liver obtained for mitochondrial evaluation had normal histology and electron microscopy including of the mitochondrial architecture, and skin biopsy electron microscopy was normal without evidence of storage products. Nextgen sequencing of mitochondrial DNA showed normal sequence

without evidence for deletions[29]. Clinical exome sequencing was reported as negative without pathogenic variants identified in known disease-causing genes.

Subject II-2, the older sister, was generally healthy, but developed migraines 5 months prior to presentation. At age 8 years, she developed a fever, nausea and vomiting, and rapidly became comatose with apnea requiring intubation. She had a large anion gap metabolic acidosis with elevated lactate (peak 22 mmol/L) with lactate/pyruvate ratio 51, with otherwise normal blood values. She was tachycardic but otherwise had normal cardiovascular function. She had depressed encephalopathic function on EEG with spike-waves over the left frontal area. She died three days later.
On brain MRI she had restricted diffusion of the left frontoparietal cortex (Figures 3D-E, white arrows) and right frontal cortex (not labeled). She had restricted diffusion of caudate nuclei and putamina (Figure 3E). MRS of the right basal ganglia revealed a large lactate inverted doublet, increased choline and reduced N-acetylaspartate signal (Figure 3F, white notched arrowhead).

Family B. Subject II-3 is a male child born to consanguineous parents of Turkish descent (cousins three times removed), who has two healthy sisters (Figure 2B). At age 4 4/12 years, following gastroenteritis with diarrhea and 48 hours fasting, he presented encephalopathic with decreased consciousness (GCS 12), dyskinesia and mydriasis. On admission, he had mild hypoglycemia 50 mg/dL, mild hyperammonemia 100 µM, and metabolic acidosis (pH 7.23, bicarbonate 12 mmol/L, base excess –14 mmol/L) with elevated lactate 6.0 mmol/L, and large ketones in urine. He had elevated creatine phosphokinase, myoglobin, and transaminases. Urine organic acids showed elevated lactate, ketones

and dicarboxylic acids. Serum acylcarnitine profile was consistent with ketosis, and plasma amino acids showed elevations of glutamine, lysine, proline, alanine, methionine and tyrosine with low citrulline, whereas CSF amino acids were generally normal (Supplemental Table 2). Brain MRI showed lesions of the splenium of the corpus callosum (Figure 3G, white arrows), felt to be clinically and radiographically consistent with mild encephalitis/encephalopathy with reversible splenial lesion (MERS). He improved with supportive therapy with intravenous glucose and vitamins, and respiratory support was not required after 2 days. Neurological signs of ptosis, strabismus and ataxia persisted for a few months before recovering, and the MRI lesions resolved after four months (not shown).

At age 5 6/12 years, following diarrhea, fever and fasting for 24 hours, he presented again encephalopathic with decreased consciousness (GCS 10), mild hypoglycemia 56 mg/dL, metabolic acidosis (pH 7.3, bicarbonate 14.2 mmol/L), elevated serum lactate 6.5 mmol/L, and in urine elevated lactate, ketones and dicarboxylic acids. Plasma ammonia and muscle enzymes remained normal. He recovered again with intravenous glucose administration. He was stable for several years but had learning difficulties and unilateral hearing loss.

At age 13 6/12 years, he had headache, asthenia and anorexia for 36 hours, and became stuporous without metabolic abnormalities. Brain MRI demonstrated hyperintense lesions on T2-weighted imaging of the caudate nuclei and putamina (Figures 3H-I, white arrowheads), and the ventromedial aspects of the thalami (Figure 3I, white notched arrowheads). Clinically, he recovered completely within two weeks. He has remained stable and generally healthy, except for easy fatigue and learning difficulties with memory and attention deficit.

A fasting test performed outside an acute episode showed normal ketogenesis. Fibroblasts showed normal enzyme activities of pyruvate carboxylase and succinyl-CoA:3-keto acid coenzyme A transferase (SCOT), and leucocytes had normal pyruvate dehydrogenase activity. Molecular analysis of *SLC19A3* and *DLD* was normal. Methemoglobin levels were borderline elevated 2.1 % and 2.9 % (normal < 2%).

Mitochondrial functional studies:

In subject A.II-3, analysis of the respiratory chain enzyme complexes during an acute episode showed markedly reduced complex IV activity with mildly decreased complex II activity, more so in muscle than in liver (Table 1). Surprisingly, blue native PAGE analysis in muscle and liver showed only a mild decrease in complex IV activity within the range of normal variation (Figure 4A), suggesting that it affected enzymatic activity more than the structure or amount of the complex. In fibroblasts, analysis of mitochondrial function was not possible as cells from subject A.II-3 rapidly died on initial culture of unknown cause. Fibroblasts from subject B.II-3 grew well and both respiratory chain enzyme activities and blue native PAGE with in-gel activity staining were normal (Supplemental Table 3). We next evaluated directly if the reduced activity evident in muscle and liver of subject A.II-3 was due to a decrease in complex IV assembly. Despite the strong decrease in complex IV activity, the amount of a protein COXIV, as a representative of complex IV subunits, was normal (Figure 4B). Following separation on a non-denaturing gel, normal amounts of fully assembled complex IV were present in both muscle and liver in the patient compared to three controls (Figure 4C). The integrity of complex I assessed by the amount of NDUFB8 as a marker subunit protein was normal, as was its assembly assessed on a non-

denaturing gel was normal (Figure 4D). Thus, the marked decrease in complex IV activity was not caused by a problem in complex IV biogenesis but rather its function.

Genetic studies

The *SQOR* gene has 8 transcripts. The main protein coding transcript *SQOR*-201 has 10 exons. The transcript has 1701 bp and encodes a protein of 450 residues (Uniprot Q9Y6N5). Whole exome studies in the proband A.II-3 showed a homozygous missense variant NM_021199.4:c.637G>A, p.(Glu213Lys) in exon 5 of the *SQOR* gene, genomic coordinates: hg19:chr15:45965982G>A, which was confirmed by Sanger sequencing (Figure 2C). Her sister A.II-2 was also homozygous for this variant and both parents and two unaffected siblings were heterozygous carriers (Figure 2A). Mutation Taster predicted this variant to be disease-causing, Polyphen2 rated it as "possibly damaging" (score 0.915), and the scaled CADD score was 34 (raw score 5.03). The *SQOR* p.Glu213Lys variant is not reported in 1000 genomes or ExAC. In gnomAD it was present in only one non-Finnish European allele (minor allele frequency (MAF) in this population $0.9x10^{-5}$, MAF $0.4x10^{-5}$ in all populations). Phylogenetically, in most species this amino acid is an acidic residue, either a glutamic acid or an aspartic acid; the mutation changes Glu213 to a basic lysine.

Whole exome sequencing in subject B.II-3 revealed a homozygous 1 bp deletion c.446delT, p.(Leu149Argfs*18), genomic coordinates chr15:45962165delT, in exon 3 of the *SQOR* gene, which was confirmed by Sanger sequencing (Figure 2C). This change predicts a loss of SQOR protein function possibly by nonsense-mediated decay of the mutant RNA or by introducing a frameshift leading to a premature truncation of protein translation. This variant was present in heterozygous state in gnomAD

only once (MAF in this population $3.98x10^{-6}$). Sanger sequencing revealed this change also in a homozygous state in the asymptomatic sisters B.II-1 and B.II-2 (Figure 2B).

SQOR functional studies

To understand the impact of the mutation on the protein, the missense variant was mapped on the crystal structure of human SQOR (Figure 2D). In the structure, Glu-213 is remote from the active site, but resides in an α-helix and is proximal to Arg-217 on the same helix and Arg-222 on an adjacent α-helix. The side chain of Glu213 is predicted to be involved in hydrogen bonding interactions with the side chains of these two arginine residues (Figure 2D). Introduction of the positively charged lysine in the Glu213Lys mutant is predicted to disrupt these electrostatic interactions and destabilize the tertiary structure of the protein. This structure suggests that the Glu213Lys variant is likely to impair protein stability rather than affect the catalytic mechanism.

Indeed, attempts to express the recombinant Glu213Lys human SQOR protein in *E. coli* using the methods employed for wild type proteins[17] as well as several modifications to growth and purification conditions, repeatedly resulted in the majority of the recombinant protein aggregating in inclusion bodies. The yield of soluble Glu213Lys SQOR protein was very low and the protein appeared to be devoid of FAD as assessed by the lack of an associated UV-visible absorption spectrum.

Western blot analysis showed very low levels of SQOR protein in muscle and liver tissues of subject A.II-3 and in fibroblasts of subject B.II-3 each compared to three controls (Figure 2E).

To evaluate the functional impact, an SQOR enzyme activity assay using sulfite as acceptor was developed using liver tissue mitochondrial membrane fractions. The initial rate was linearly dependent

on lysate protein concentration over the range of 0.064 to 0.698 mg protein/mL (final concentration) (r^2 = 0.98) (Supplemental Figure 1A). A K_M of 2.2±1.1 mM for sulfide and a V_{max} of 27.8±8.9 nmol.min^{-1}.mg protein^{-1} at 37°C were observed (Supplemental Figure 1C). The V_{max} value was obtained at sulfite concentrations of around 1-2 mM (Supplemental Figure 1D), and at coenzyme Q_1 concentrations of 100 µM (Supplemental Figure 1E). The coefficient of variation (COV) in the same liver tissue sample was 14%. SQOR activity in subject A.II-3 liver was severely reduced to 6% of the average of control values (0.71±0.57 vs. 11.42±3.75 nmol.min^{-1}.mg protein^{-1}, normal range 7.56-16.94; n=5) (Supplementary figure 2A).

To facilitate future diagnosis of SQOR deficiency, the enzyme assay was modified for use with fibroblasts and PBMCs. In fibroblasts, the initial rate of enzyme activity was linear over a lysate protein concentration range from 0.01 to 0.34 mg protein.mL^{-1} (r^2=0.98) (Supplemental Figure 1B). With control fibroblasts, a specific activity of 82.1±21.2 nmol.min^{-1}.mg protein^{-1} (normal range 51.6-115.2; n=12), COV 26% was obtained, whereas subject B.II-3 fibroblasts had SQOR activity of 0.41±0.16 nmol.min^{-1}.mg protein^{-1}, 0.49% of average control value (Supplemental Figure 2B). Analysis of control PBMCs yielded a specific activity of 43.6±2.1 nmol.min^{-1}.mg protein^{-1} (n=8), COV 5%. Additional family members who were found to be carriers for this mutation had 62%, 66%, and 42% of mean control enzyme activity in PBMCs.

The homozygosity of the patient and the identification of additional carriers in distant family members suggested that Glu213Lys may represent a founder mutation. Targeted mutation screening of de-identified DNA samples of 40 subjects from this population identified three carriers (carrier frequency p=0.08±0.04), implying an affected incidence of 1 in 711. Untargeted population analysis of the gnomAD

database using predictive software estimated a carrier frequency of p=0.0023 (1 in 215), implying an incidence of 1 in 184,477 for biallelic pathogenic variants.

DISCUSSION

The Glu213Lys variant replaces an acidic with a basic amino acid disrupting hydrogen bonding interactions and destabilizing the SQOR protein. This protein instability resulted in strongly reduced protein levels and severely decreased enzyme activity, but not its complete absence. The protein instability severely limited bacterial expression of the recombinant Glu213Lys human SQOR enzyme. These functional data confirm bioinformatic predictions that this variant is pathogenic. It tracks with deficient enzyme activity in the family and represents a founder variant in the Lehrerleut Hutterite population with a carrier frequency estimated to be as high as 1 in 13 based on limited screening of samples from this population. The frameshift mutation in Family B likewise resulted in severely reduced SQOR protein and enzyme activity. These pathogenic variants limited the ability of the patient to metabolize H_2S, and presumably resulted in episodic accumulation.

In all patients, acute symptoms were triggered by infections and fasting, episodes associated with protein catabolism. Outside acute events, our patients generally appeared healthy, and likewise two siblings in Family B have remained asymptomatic for prolonged time. They did not exhibit symptoms such as chronic gastrointestinal upset or a tendency for petechiae that have previously been attributed to excess H_2S in patients with pathogenic variants in *ETHE1* resulting in deficient persulfide dioxygenase

activity, the next step in the pathway[4]. In contrast to *ETHE1* deficiency, ethylmalonic acid was not noted in urine organic acid analysis, supporting that the inhibition of short chain acyl-CoA dehydrogenase could be due to accumulating coenzyme A-persulfide in the intact SQOR protein in *ETFE1* deficiency, but not in *SQOR* deficiency[27]. Chronic loss of complex IV protein attributed to excess H_2S in the mouse model of *ETHE1* was also not observed in our patient[5]. Rather, a functional deficiency of complex IV activity was seen, while the levels and assembly of complex IV appeared comparable to controls. Deficient complex IV activity results in an acute energy defect which in brain usually presents as Leigh disease[21], although some genetic causes also include myopathy or cardiomyopathy (e.g. *SCO2*)[30]. In our patients, the cardiovascular system appeared to be relatively spared with cardiovascular symptoms limited to transient hypotension and shock present only in the context of multiorgan failure, which recovered with supportive care. Acute H_2S toxicity causes depression in cardiac contractility and pulseless electrical activity[31]. In an animal model of acute H_2S intoxication leading to 75% mortality, 25% of surviving animals had neurological lesions of neuronal necrosis of the cortex, putamen and thalamus, which closely resembles the symptoms noted in patient A.II-2[31]. The striking involvement of the hippocampus and mammillary body in patient A.II-3 without prolonged seizures likely represents the SQOR deficiency rather than an injury secondary to her poor state. In mouse, SQOR protein is present in the hippocampus (Maclean, unpublished observation). Given the long asymptomatic period in subject A.II-2 and subjects B.II-1 and B.II-2, we consider it possible that undiagnosed patients exist, including in the Hutterite population.

The presence of normal amounts of cytochrome c oxidase complex but severely reduced activity, indicates that the fundamental pathophysiological mechanism of SQOR deficiency appears to be due to the resulting accumulation of toxic metabolites, rather than disruption of complex IV biogenesis. Acute illness is associated with catabolism and associated endogenous protein breakdown. The resulting increase in cysteine can increase H_2S generation, which would accumulate in the absence of sufficient SQOR enzyme activity. At high levels, H_2S can coordinate to the iron in the heme a group of complex IV resulting in strong inhibition[3]. The complete absence of SQOR in yeast impaired growth under obligate aerobic conditions, whereas mutants that retain low levels of activity restored oxidative growth, consistent with the detoxifying role attributed to SQOR[32]. We hypothesize that in our patients, the low residual SQOR activity was likely sufficient to support H_2S clearance during stable episodes but was insufficient during acute illness with catabolism resulting in H_2S accumulation and toxicity.

During acute H_2S intoxication, two pools accumulate: a soluble and diffusible pool of hydrogen sulfide gas in equilibrium with the sulfide (HS^-) anion, and a pool of sulfide bound to metallo-proteins (e.g. hemes) and cysteine residues in a variety of proteins[33,34]. It is unclear to what extent these cysteine adducts can form non-enzymatically in the absence of functional SQOR. The toxicity mechanism in our patients might be partially different from that of acute exogenous H_2S intoxication. In our patient A.II-3, the more severe reduction in complex IV activity was noted in muscle tissue, where the sulfide generating enzymes could not be detected, compared to liver tissue where the enzymes were present and unchanged versus controls (Supplemental Figure 2). This illustrates the importance of great diffusibility of H_2S, which is more soluble and diffusible than oxygen or carbon dioxide[33]. A large pool of

H_2S bound to ferrous myoglobin has been proposed to explain the sensitivity of muscle tissue to H_2S toxicity[35]. SQOR has a wide tissue distribution including in neurons, oligodendrocytes and vascular endothelial cells in brain, likely reflecting a need to protect against this toxin that readily diffuses across membranes[36,37]. Rapid diffusion of H_2S from tissue culture medium can explain the normal complex IV activity in cultured fibroblasts.

Recognition of the enzymatic basis and intoxication of the respiratory chain in the pathophysiology of SQOR deficiency opens up possible therapeutic opportunities. First, reduction in H_2S production should be pursued. Since the majority of H_2S is generated from cysteine catabolism in the body and gut microbiome[13], limiting dietary cysteine and aggressive prevention of episodes triggering catabolism by adequate provision of calories and avoidance of prolonged fasting can be considered. Catabolic episodes likely triggered the acute crisis in our patients. H_2S is produced by γ-proteobacteria including certain gram-negative and *Clostridia* species, which can be increased by omeprazole or lansoprazole[14], and can be therapeutically reduced by treatment with metronidazole, similar to the treatment of ETHE1 disorder[38]. Certain vegetables, such as garlic, onions, and certain cruciferous vegetables, contain organic polysulfides, which can directly release hydrogen sulfide and could be avoided[14]. Next, the toxic effects of accumulated H_2S could be mitigated. Toxicological studies have shown that hydroxocobalamin can bind H_2S and pharmacological doses have been used for detoxification during acute H_2S poisoning, similar to the treatment of cyanide which shares a similar pathophysiology[33,34,39]. During acute symptomatic periods in illness, acute administration of very high doses of hydroxocobalamin (70 mg/kg) may be required. Given the rapidity of onset of life-threatening events, which in our patients occurred

within hours, preventive daily subcutaneous administration of pharmacologic doses of hydroxocobalamin, as is used to treat cobalamin C disorder, should be considered. Further, methylene blue has been shown to reduce mortality due to acute H_2S poisoning by reducing its mitochondrial toxicity[31.40].

In summary, we describe a new genetic cause of Leigh disease associated with pathogenic variants in *SQOR*, whereby intermittent accumulation of H_2S results in acute isolated complex IV deficiency. We developed an enzyme assay that allows non-invasive measurement of the enzyme activity, which is useful for diagnosis. Recognition of SQOR deficiency as a cause of Leigh diseases is clinically important since it suggests several treatment modalities to prevent neurological complications.

Acknowledgments

We acknowledge financial support from Children's Hospital Colorado Foundation, Summits for Samantha and Miracles for Mito (JVH, MWF, AAL). The study was also supported by the NIH grants R35GM130183 to RB, and F32GM122357 to APL, and by NIH/NCATS Colorado CTSA Grant Number UL1 TR002535. Contents are the authors' sole responsibility and do not necessarily represent official NIH views.

LED was the recipient of a Child Health Research Internship at the CU Anschutz campus, which is supported by the Daniel and Janet Mordecai Foundation, Department of Pediatrics and the Research Institute, Children's Hospital Colorado. KNM gratefully acknowledges financial support from the William R. Hummel Homocystinuria Research Fund and holds the Ehst-Hummel-Kaufmann Family Endowed

Chair in Inherited Metabolic Disease. Sequencing performed at the University of Colorado was performed by the Molecular Biology Unit of the Barbara Davis Center for BioResources Core Facility, which receives support from the Children's Diabetes Foundation, the Davis trust, and the UC-AMC Strategic Infrastructure for Research Committee. TBH was supported by the German Bundesministerium für Bildung und Forschung (BMBF) through the Juniorverbund in der Systemmedizin "mitOmics" (FKZ 01ZX1405C to TBH), the intramural fortüne program (#2435-0-0) and by the Deutsche Forschungsgemeinschaft (DFG, German Research Foundation) – Projektnummer (418081722). The Montana Genetics Program at Shodair Children's Hospital is supported by the Montana Department of Public Health and Human Services (PHH18-0157JT MT Clinical Genetics Program). Funding sources had no role in the design or execution of the study, the interpretation of data, or the writing of the study.

REFERENCES

1. Kolluru GK, Shen X, Bir SC, Kevil CG. Hydrogen sulfide chemical biology: pathophysiological roles and detection. Nitric Oxide 2013;35:5-20.

2. Kabil O, Vitvitsky V, Banerjee R. Sulfur as a signaling nutrient through hydrogen sulfide. Annu. Rev. Nutr 2014;34:171-205.

3. Cooper CE, Brown GC. The inhibition of mitochondrial cytochrome oxidase by the gases carbon monoxide, nitric oxide, hydrogen cyanide and hydrogen sulfide: chemical mechanism and physiological significance. J. Bioenerg. Biomembr. 2008;40:533-539.

4. Tiranti V, Viscomi C, Hildebrandt T, Di Meo I, Mineri R, Tiveron C, Levitt MD, Prelle A, Fagiolari G, Rimoldi M, Zeviani M. Loss of ETHE1, a mitochondrial dioxygenase, causes fatal sulfide toxicity in ethylmalonic encephalopathy. 2009;15:200-205.

5. Di Meo I, Fagiolari G, Prelle A, Viscomi C, Zeviani M, Tiranti V. Chronic exposure to sulfide causes accelerated degradation of cytochrome c oxidase in ethylmalonic encephalopathy. Antiox. Redox Sign. 2011;15:353-362.

6. Hildebrandt TM, Di Meo I, Zeviani M, Viscomi C, Braun H-P. Proteome adaptations in Ethe1-deficient mice indicate a role in lipid catabolism and cytoskeleton organization via post-translational modification. Biosci. Rep. 2013;33:575-584.

7. Di Meo I, Lamperti C, Tiranti V. Mitochondrial diseases caused by toxic compound accumulation: from etiopathology to therapeutic approaches. EMBO Mol. Med. 2015;7:1257-1266.

8. Luna-Sánchez M, Hidalgo-Gutiérrez A, Hildebrandt TM, Chaves-Serrano J, Bariocanal-Casado E, Santos-Fandila Á, Romero M, Sayed RKA, Duarte J, Prokisch H, Schuelke M, Distelmaier F, Escames G, Acuña-Castroviejo D, López LC. CoQ deficiency causes disruption of mitochondrial sulfide oxidation, a new pathomechanism associated with this syndrome. EMBO Mol. Med. 2017;9(1):78-95.

9. Ziosi M, Di Meo I, Kleiner G, Gao X-H, Barca E, Sanchez-Quintero MJ, Tadesse S, Jiang H, Qiao C, Rodenburg RJ, Scalais E, Schuelke M, Willard B, Hatzoglou M, Tirnati V, Quinzi CM. Coenzyme Q deficiency causes impairment of the sulfide oxidation pathway. EMBO J. 2017;9(1):96-111.

10. Chiku T, Padovani D, Zhu W, Singh S, Vitvitsky V, Banerjee R. H_2S Biogenesis by human cystathionine γ-lyase leads to the novel sulfur metabolites lanthionine and homolanthionine and is responsive to the grade of hyperhomocysteinemia. J. Biol. Chem. 2009;284:11601-11612.

11. Singh S Padovani D, Leslie RA, Chiku T, Banerjee R. Relative contributions of cystathionine β-synthase and γ-cystathioninase to H_2S biogenesis via alternative trans-sulfuration reactions. J. Biol. Chem. 2009;284:22457-22466.

12. Yin J, Ren W, Yang G, Duan J, Huang X, Fang R, Li C, Li T, Yin Y, Hou Y, Kim SW. L-cysteine metabolism and its nutritional implications. Mol. Nutr. Food Res. 2016;60:134-146.

13. Magee E A, Richardson C J, Hughes R, Cummings J H. Contribution of dietary protein to sulfide production in the large intestine: an in vitro and a controlled feeding study in humans. Am. J. Clin. Nutr. 2000;72:1488-1494.

14. Wallace J L, Motta J P, Buret A G. Hydrogen sulfide: an agent of stability at the microbiome-mucosa interface. Am. J. Physiol. Gastrointest. Liver Physiol. 2018;314:G143-G149.

15. Libiad M, Vitvitsky V, Bostelaar T, Bak D W, Lee H-J, Sakamoto N, Fearon E, Lyssiotis C A, Weerapana E, Banerjee R. Hydrogen sulfide perturbs mitochondrial bioenergetics and triggers metabolic reprogramming in colon cells. J. Biol. Chem. 2019; 294(13):12077-12090

16. Jackson MR, Melideo SL, Jorns MS. Human sulfide:quinone oxidoreductase catalyzes the first step in hydrogen sulfide metabolism and produces a sulfane sulfur metabolite. Biochemistry 2012;51:6804-6815.

17. Libiad M, Yadav PK, Vitvitsky V, Martinov M, Banerjee R. Organization of the human mitochondrial hydrogen sulfide oxidation pathway. J. Biol. Chem. 2014;289:30901-30910.

18. Landry AP, Ballou DP, Banerjee R. H_2S oxidation by nanodisc-embedded human sulfide quinone oxidoreductase. J. Biol. Chem. 2017;292:11641-11649.

19. Rahman S, Blok R B, Dahl H H, Danks D M, Kirby D M, Chow C W, Christodoulou J, Thorburn D R. Leigh syndrome: clinical features and biochemical and DNA abnormalities. Ann. Neurol. 1996;39(3):343-351.

20. Lake N J, Compton A G, Rahman S, Thorburn D R. Leigh syndrome: one disorder, more than 75 monogenic causes. Ann. Neurol. 2016;79(2):190-203.

21. DiMauro S, Servidei S, Zeviani M, DiRocco M, DeVivo D C, DiDonato S, Uziel G, Berry K, Hoganson G, Johnson S D, Johnson P C. Cytochrome c oxidase deficiency in Leigh syndrome. Ann. Neurol. 1987;22:498-506.

22. Karczewski K J, Francioli L C, Tiao G, Cummings B B, Alföldi J, Wang Q, Collins R L, Laricchia K , et al. The Genome Aggregation Database Consortium, Neale B M, Daly M J, MacArthurs D G. Variation across 141,456 human exomes and genomes reveals the spectrum of loss-of-function intolerance across human protein-coding genes. BioRxiv doi https://doi.org/10.1101/531210

23. Chatfield K C, Coughlin C R 2nd, Friederich M W, Gallagher R C, Hesselberth J R, Lovell M A, Ofman R, Swanson M A, Thomas J A, Wanders R J, Wartchow E P, Van Hove J LK. Mitochondrial energy failure in HSD10 disease is due to defective mtDNA transcript processing. Mitochondrion 2015;21:1-10.

24. Friederich M W, Erdogan A J, Coughlin C R II, Elos M, Jiang H, O'Rourke C, Lovell M A, Wartchow E, Gowan K, Chatfield K C, Chick W, Spector E, Van Hove J L K, Riemer J. Mutations in the accessory subunit NDUFB10 result in isolated complex I deficiency and illustrate the critical role of intermembrane space import for complex I holoenzyme assembly. Hum. Mol. Genet. 2017;26(4):702-716.

25. Maclean K N, Jiang H, Greiner L S, Allen R H, Stabler S P. Long-term betaine therapy in a murine model of cystathionine beta-synthase deficient homocystinuria: decreased efficacy over time reveals a

significant threshold effect between elevated homocysteine and thrombotic risk. Mol. Genet. Metab. 2012;105(3):395-403.

26. Banerjee R, Chiku T, Kabil O, Libiad M, Motl N, Parmod K. Assay methods for H2S biogenesis and catabolism enzymes. Methods Enzymol. 2015;554:189-200.

27. Landry AP, Moon S, Kim H, Yadav PK, Guha A, Cho US, Banerjee R. A catalytic trisulfide quinone oxidoreductase catalyzes coenzyme A persulfide synthesis and inhibits butyrate oxidation. Cell Chem Biol. 2019;26:1515-1525.

28. Schrödinger, LLC. The PyMOL Molecular Graphics System, Version 2.0, accessed at https://pymol.org (2019).

29. Zhang W, Cui H, Wong LJ. Comprehensive one-step molecular analyses of mitochondrial genome by massively parallel sequencing. Clin Chem 2012;58(9):1322-1331.

30. Rak M, Bénit P, Chrétien D, Bouchereau J, Schiff M, El-Khoury R, Tzagaloff A, Rustin P. Mitochondrial c oxidase deficiency. Clin. Sci. (lon) 2016;130(6):393-407.

31. Haouzi P, Sonobe T, Judenherc-Haouzi A. Developing effective countermeasures against acute hydrogen sulfide intoxication: challenges and limitations. Ann. N. Y. Acad. Si. 2016;1374:29-40.

32. Vande Weghe J G, Ow D W. A fission yeast gene for mitochondrial sulfide oxidation. J. Biol. Chem. 1999;274:13250-13257.

33. Haouzi P, Sonobe T, Judenherc-Haouzi A. Developing effective countermeasures against acute hydrogen sulfide intoxication: challenges and limitations. Ann. N. Y. Acad. Si. 2016;1374:29-40.

34. Haouzi P, Sonobe T, Torsell-Tubbs N, Prokopczyk B, Chenuel B, Klingerman C M. *In vivo* interactions between cobalt and ferric compounds and the pools of sulphide in the blood during and after H_2S poisoning. Toxicol. Sci. 2014;141(2):493-504.

35. Bostelaar T, Vitvitsky V, Kumutima J Lewis B E, Yadav P K, Brunold T C, Filipovic M Lehnert N, Stemler TL, Stemmler TL, Banerjee R. Hydrogen sulfide oxidation by myoglobin. J. Am. Chem. Soc. 2016;138(27):8476-8488.

36. Ackermann M, Kubitza M, Hauska G, Piña A L. The vertebrate homologue of sulfide-quinone reductase in mammalian mitochondria. Cell Tissue Res. 2014;358:779-792.

37. Ackermann M, Kubitza M, Brawanski A, Hauska G, Piña A L. The vertebrate homolog of sulfide-quinone reductase is expressed in mitochondria of neuronal tissues. Neuroscience 2011;199:1-12.

38. Viscomi C, Burlina A B, Dweikat I, Savoirado M, Lamperti C, Hildebrandt T, Tiranti V, Zeviani M. Combined treatment with oral metronidazole and N-acetylcysteine is effective in ethylmalonic encephalopathy. Nat. Med. 2010;16(8):869-871.

39. Haouzi P, Chenuel B, Sonobe T. High-dose hydroxocobalamin administered after H2S exposure counteracts sulfide-poisoning-induced cardiac depression in sheep. Clin. Toxicol. 2015;53:28-36.

40. Houzi P, Tubbs N, Chaeung J, Judenher-Haouzi A. Methylene blue administration during and after life-threatening intoxication by hydrogen sulfide: efficacy studies in adult sheep and mechanisms of action. Toxicol. Sci. 2019;168(2):443-459.

TABLES

Table 1: Respiratory chain enzyme activities in patient A.II.3

	Activity (controls) nmol.min^{-1}.mg protein^{-1}	**% of normal**	**SD**	**Activity / CS**	**SD**	**Activity / CO II**	**SD**
MUSCLE							
Complex I	44.2 (23.6-74.8)	98%	0.1	176 (98-271)	0.1	888 (285-767)	1.9
Complex II	49.8 (49.0-133.4)	56%	-1.8	198 (251-573)	-1.8	NA	NA
Complex III	20.3 (5.7-31.4)	117%	0.5	81 (19-72)	0.5	408 (45-369)	1.2
Complex II-III	45.7 (34.2-107.6)	72%	-0.7	182 (172-472)	-0.1	918 (549-1226)	0.7
Complex IV	**0.4** (1.1-3.8)	**15%**	**-4.3**	2 (4-23)	**-4.3**	**8** (11-68)	**-4.6**
Citrate synthase	251.7 (159.8-353.3)	98%	0.0	NA	NA	NA	NA
LIVER							
Complex I	60.8 (14.4-56.0)	172%	1.5	600 (162-730)	0.9	264 (68-252)	1.3
Complex II	230.1 (174.7-309.8)	99%	0.1	2269 (2304-3311)	-1.3	NA	NA
Complex III	27.6 (13.8-27.6)	145%	3.1	273 (128-315)	0.6	120 (50-118)	1.0
Complex II-III	50.0 (10.8-107.3)	85%	0.4	493 (138-1062)	-0.2	217 (62-383)	0.0
Complex IV	**0.4** (0.5-3.2)	**22%**	-1.8	**4** (6-35)	**-2.4**	**2** (3-13)	**-2.5**
Citrate synthase	101.4(59.5-109.3)	120%	0.1	NA	NA	NA	NA

Legend: The activities in muscle and liver tissue of each respiratory chain complex and of the combined complex II-III are shown expressed as nmol.min^{-1}.mg protein^{-1} and as a ratio of the activity over citrate synthase activity (activity/CS) and as a ratio over the activity of complex II (activity/ Co II). The patient's values are followed by normal values in parentheses and the percentage of the average normal value is provided. The values are also expressed as standard deviations (Z-score) of the log transformed values of controls, which are normally distributed. Activities that are reduced are highlighted in bold.

Abbreviations: CS = citrate synthase, CO II = complex II.

FIGURES

Figure 1: The metabolism of hydrogen sulfide

Legend: Hydrogen sulfide (H_2S) is formed from cysteine by cystathionine β-synthase (CBS) or by cystathionine-γ-lyase (CTH), or after transamination via cysteine aminotransferase (CAT) and the action of mercaptopyruvate sulfur transferase (MPST). Cysteine is also produced by gut bacteria. Cysteine is oxidized by cysteine dioxygenase (CDO) in the pathway to taurine synthesis. H_2S is primarily oxidized by sulfide:quinone oxidoreductase (SQOR) with the electrons transferred to coenzyme Q (CoQ), and with concomitant sulfur transfer to glutathione (GSH) to form glutathione persulfide (GSSH). GSSH is then oxidized to form sulfite by persulfide dioxygenase (SDO, gene *ETHE1*), which is further oxidized to sulfate by sulfite oxidase (SUOX). GSSH can also be converted to thiosulfate by thiosulfate sulfurtransferase (TST). Accumulating hydrogen sulfide can inhibit respiration at the level of complex IV. Other abbreviations used: CoQ is oxidized coenzyme Q, CoQH2 is reduced coenzyme Q, Cytc is cytochrome c, α-KG is α-ketoglutarate, SO_3^{2-} is sulfite, SO_4^{2-} is sulfate, SSO_3^{2-} is thiosulfate. MPST is variably localized in both the mitochondria and cytosol.

Figure 2: The SQOR pathogenic variant causes lack of protein and enzyme activity

Legend: A. In family A, a homozygous pathogenic variant c.637G>A in exon 5 was identified in subjects A.II-2 and A.II-3 indicated by a filled circle, whereas subjects A.I-1, A.I-2, A.II-1 and A.II-4 are carriers for

this pathogenic variant. B. In family B, the children are each homozygous for the variant c.446delT whereas the parents are heterozygous carriers. C. Sanger sequencing results of both variants in subjects A.II-3 and B.II-3 are shown. D. The variant c.637G>A codes for p.(Glu213Lys) which is mapped on the crystal structure of the human SQOR protein (PDB: 6O1C). The human SQOR monomer is shown in grey ribbon with the flavin cofactor (yellow) and select residues (green) are shown in stick display. Glu213 is relatively surface exposed. The close-up view shows that the side chain of Glu213 interacts with Arg217 and Arg222. The Glu213Lys mutation is predicted to disrupt electrostatic stabilization of the arginine side chains. E. The SQOR protein (at approx. 50 kDa) is virtually absent in the patient liver and strongly reduced in muscle as shown by western blot, using ANT (approx. 33 kDa) as a loading control in subject A.II-3 and in fibroblast of subject B.II-3.

Figure 3: Brain magnetic resonance imaging in patients affected by SQOR deficiency

Legend: A-C. Axial diffusion-weighted brain MR images of patient A.II-3 demonstrated symmetric restricted diffusion and edema involving the basal ganglia (white arrowheads), hippocampi (white arrows), and mammillary bodies (white notched arrowheads). D-E. Axial diffusion-weighted brain MR images of patient A.II-2 reveal predominantly left-sided restricted diffusion and edema of the cerebral cortices (white arrows) and symmetric restricted diffusion and edema of the basal ganglia (white arrowheads). F. Single voxel proton MR spectroscopy (TE = 144) interrogating the left frontal lobe of patient A.II-2 shows a large inverted lactate doublet at 1.3 ppm. G. In patient B.II-3 at age 4 4/12 years, axial T2-weighted brain MRI image illustrated patchy increased signal involving the splenium of the

corpus callosum (white arrows). H-I. One year later for the same patient, axial T2-weighted brain MRI images show symmetric edema of the basal ganglia (white arrowheads) and anteromedial thalami (white notched arrowheads), all of which had reduced diffusivity (not shown).

Figure 4: Assembly and activity of mitochondrial complexes

Legend: A. Mitochondrial complexes were separated on a blue native gel and assayed with in-gel activity staining in muscle (upper panel) and in liver (lower panel). A mild decrease in complex IV staining was observed in muscle for patient A.II-3. B. In muscle and liver of patient A.II-3 a normal amount of the complex IV subunit COXIV is seen, using citrate synthase as a loading control. C. Both muscle and liver exhibit normal levels of fully assembled complex IV in patient A.II-3 compared to control samples as revealed by blue gel followed by western blotting and detection with COXIV antibody. D. The assembly of complex I is normal in patient A.II-3 compared to controls as identified by blue native gel followed by western blotting and detection with an antibody against NDUFS2.

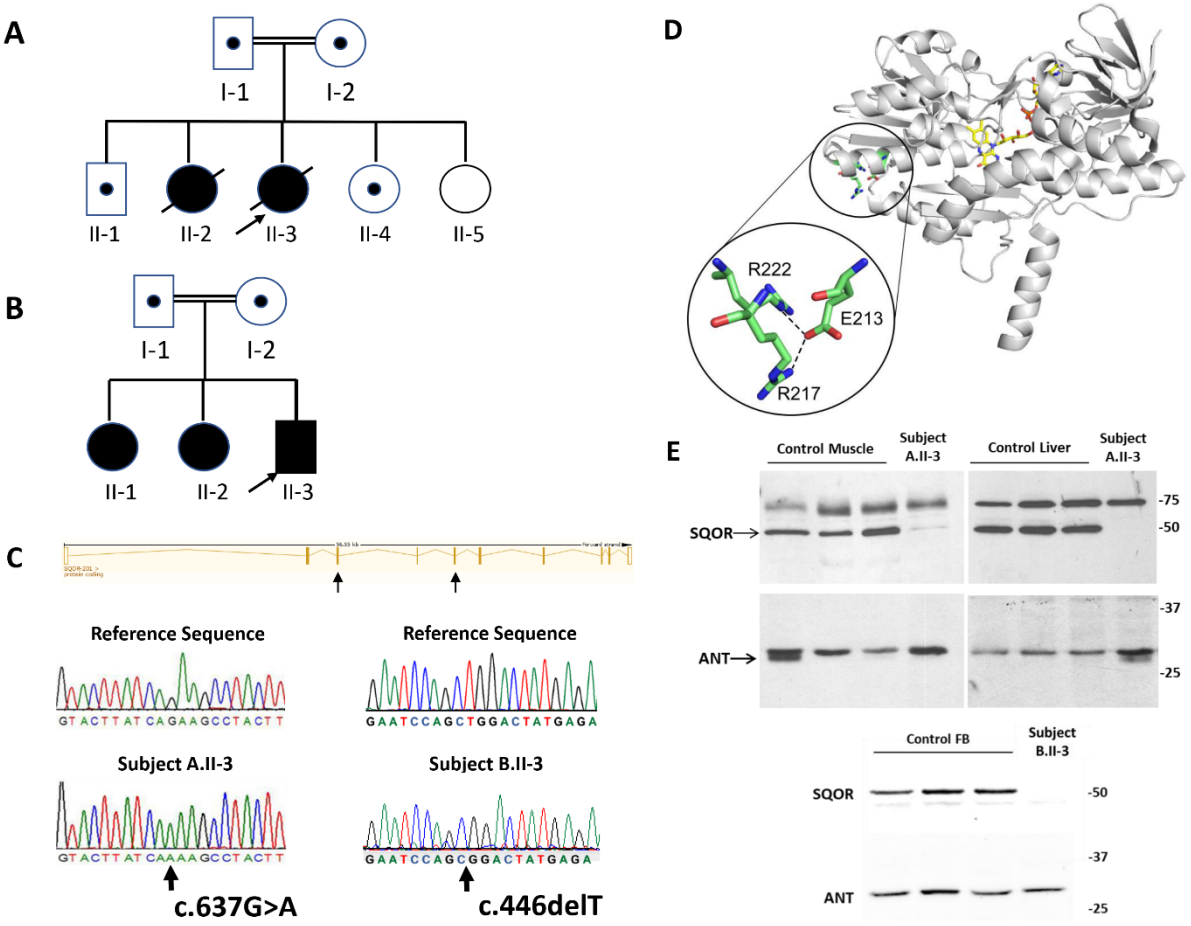

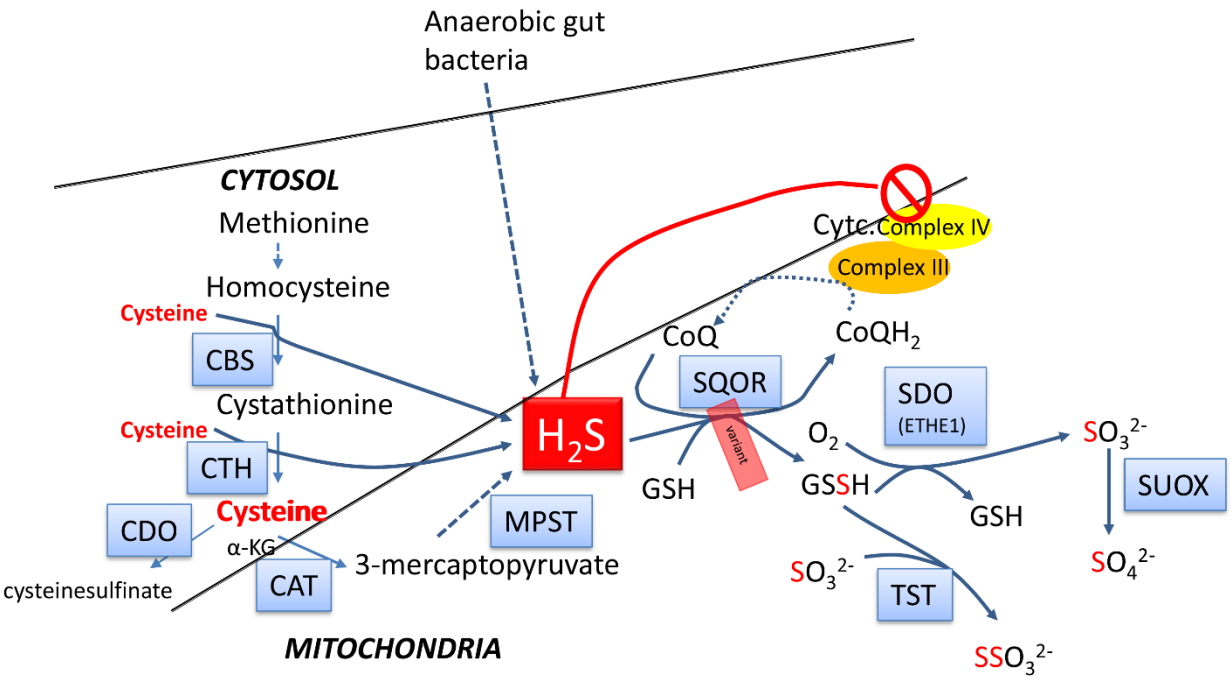

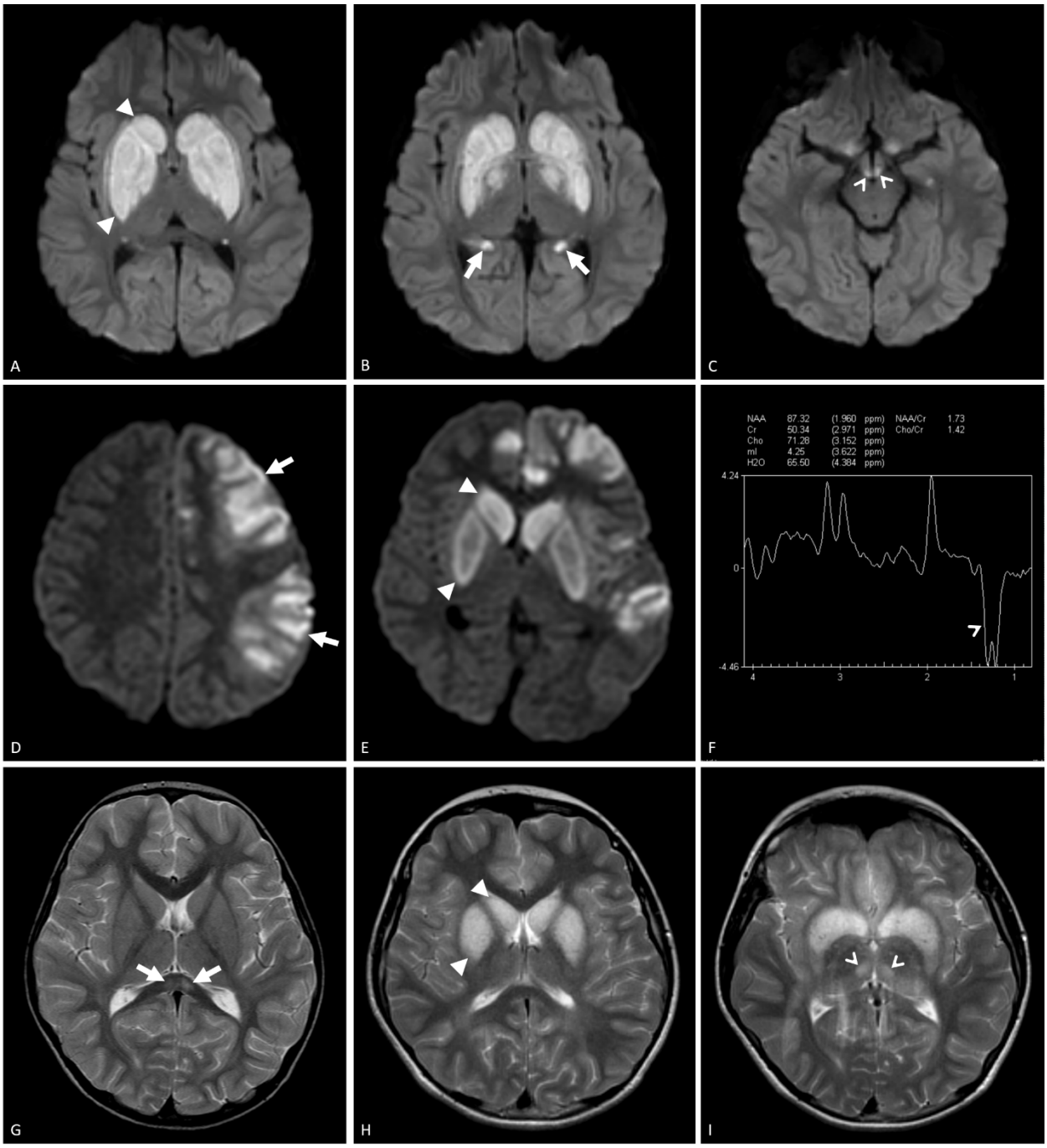

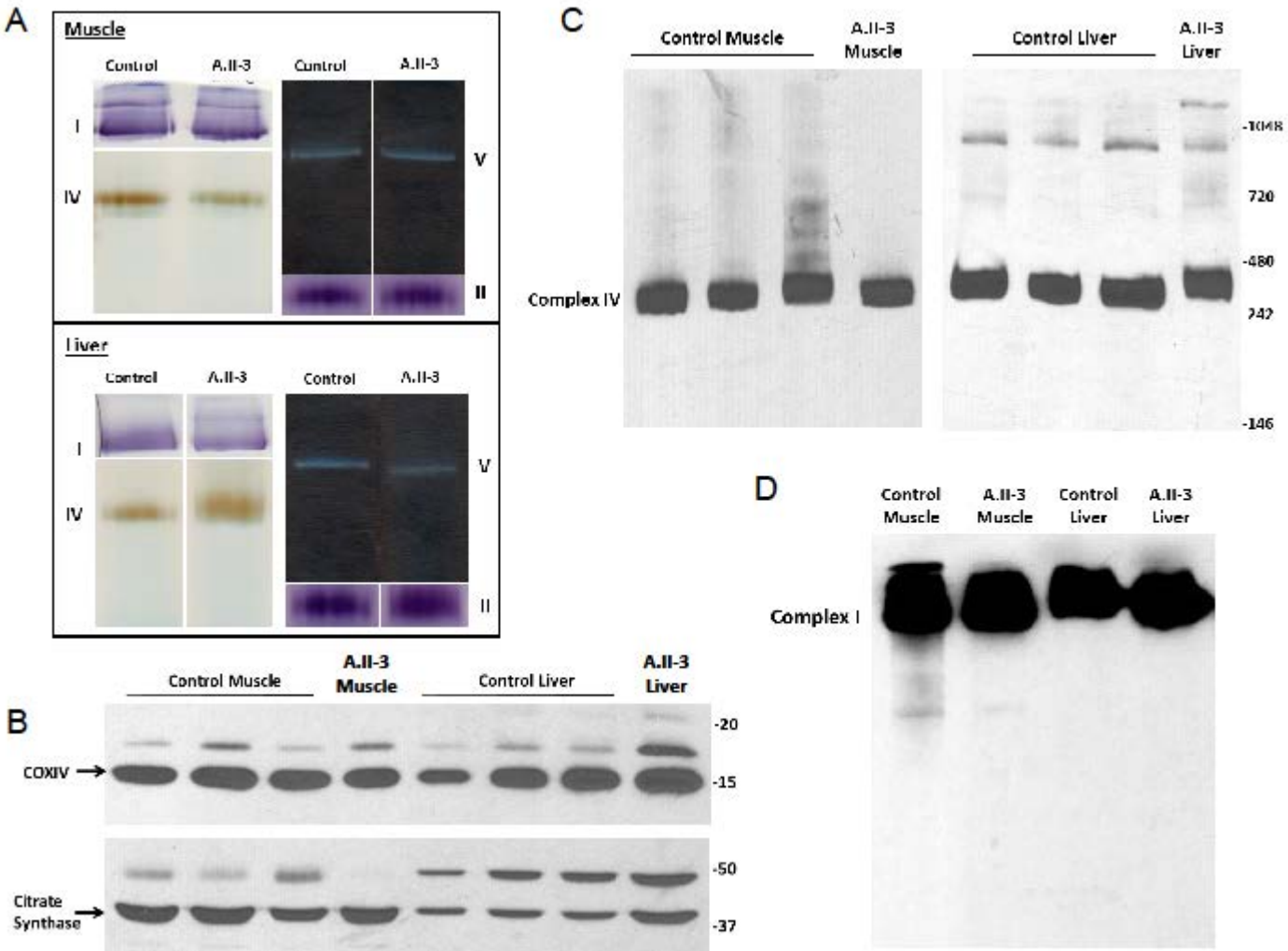

Please wait...

Please wait...

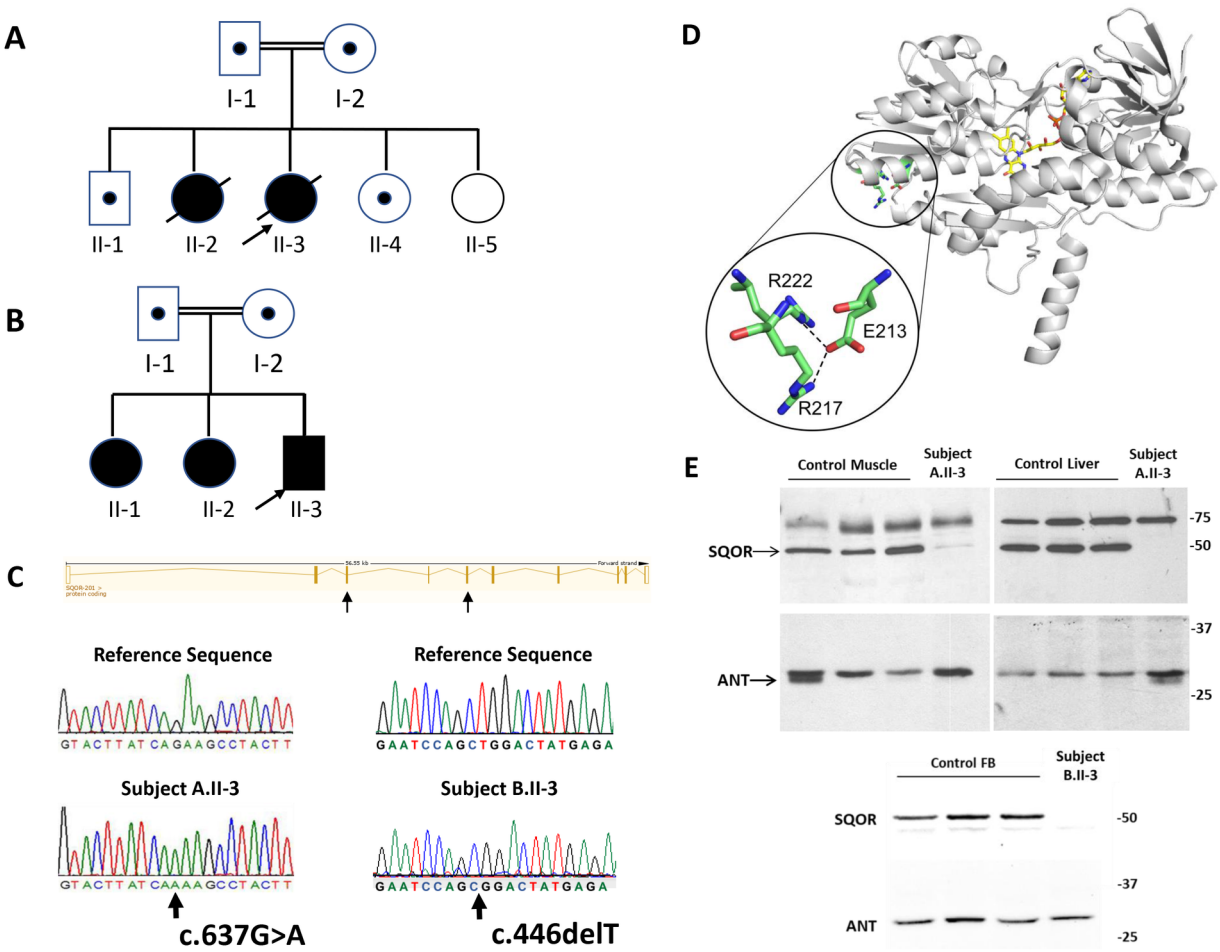

JIMD_12232_Figure2_14FEB2020.tif

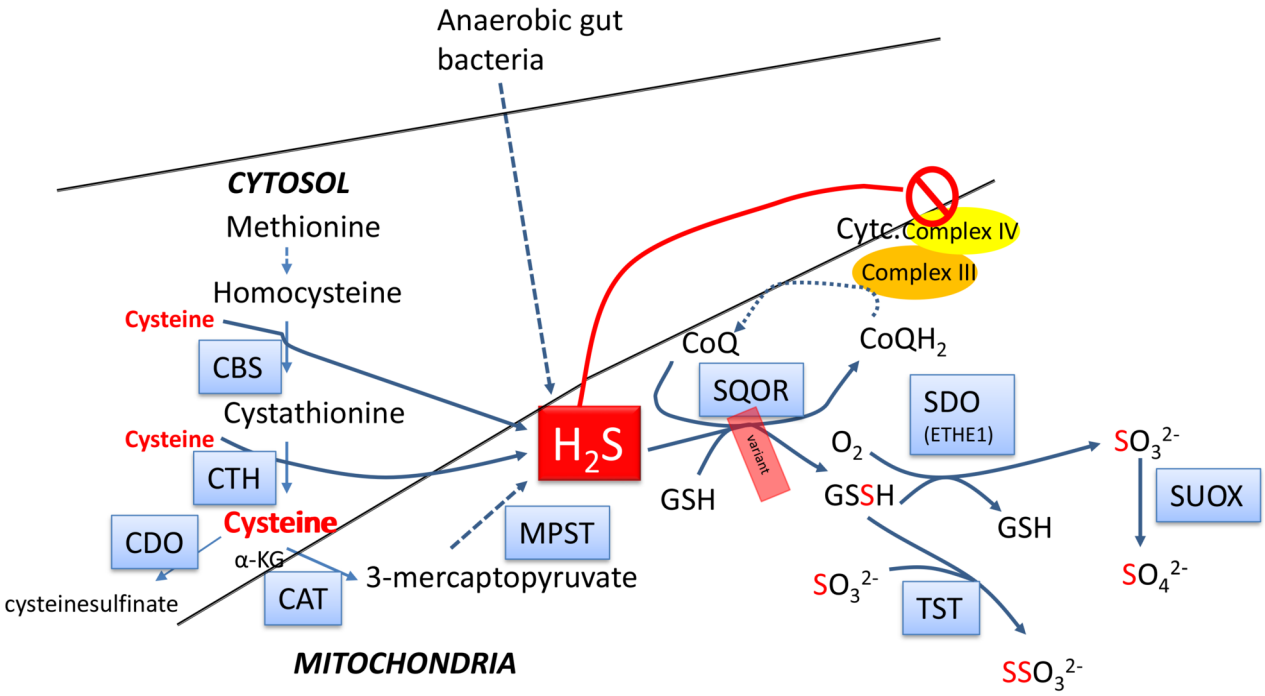

JIMD_12232_SQOR_Figure1.tif

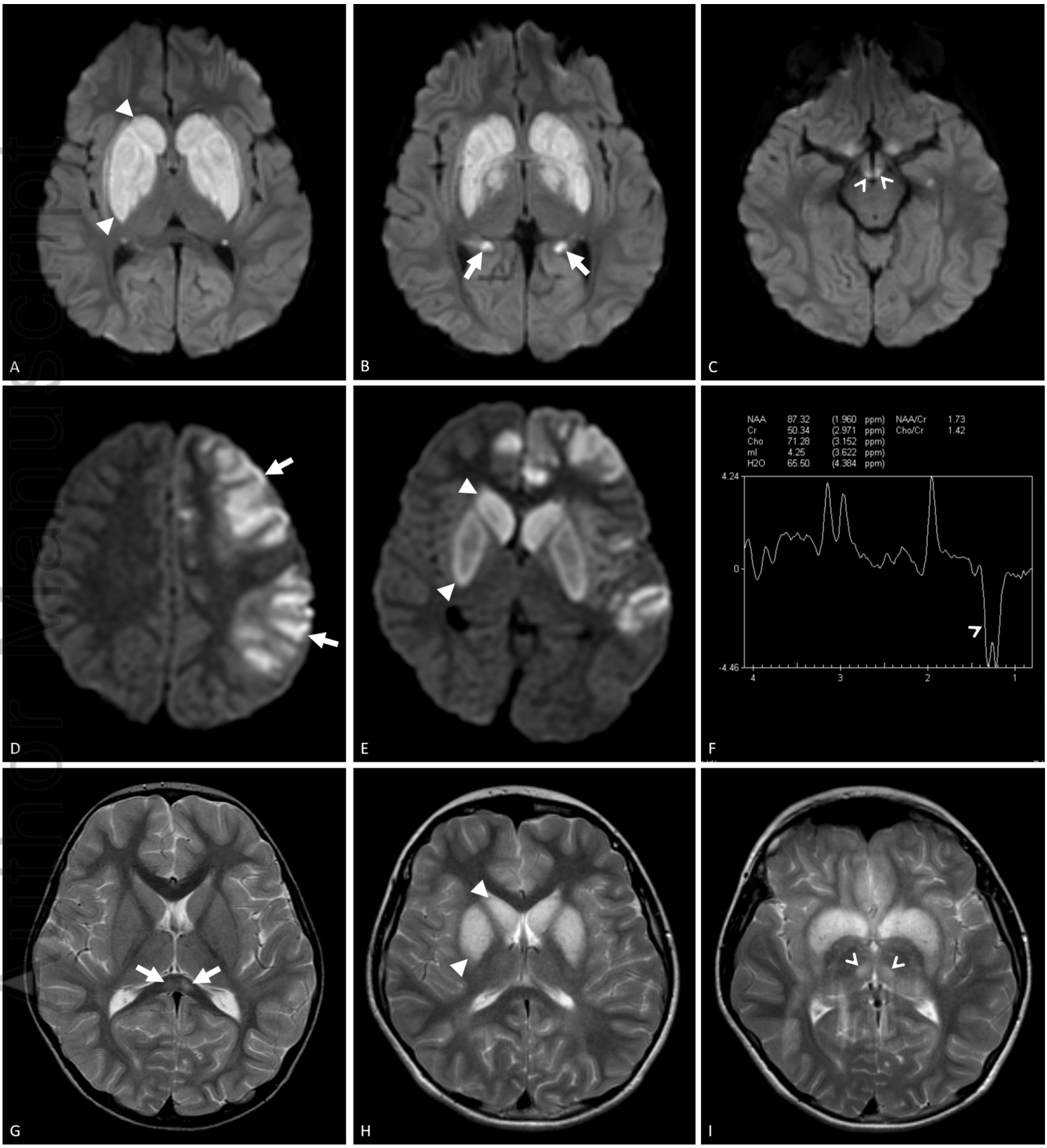

JIMD_12232_SQOR_Figure3_FEB2020.tif